# 1.1 HEXAGONAL FREE FORM SHELL SUPPORTED ON SIX VERTICES UNDER WIND PRESSURES


**Maya Sian Caycedo Garcia**

**Sebastian Moreno Cardenas**

**Antônio Mário Ferreira**

**Isaias Vizotto**

maya_sian@hotmail.com

sebastian.moreno.8026@gmail.com

bfengenharia@bfengenharia.com

vizotto@fec.unicamp.br

University of Campinas – School of Civil Engineering, Architecture and Urbanism

Av. Albert Einstein, 951 – Cidade Universitária Zeferino Vaz – Barão Geraldo

CEP 13.083-852, Campinas, SP, Brazil



***Abstract.*** *The objective of this paper is to present the results and conclusions of the research of structural behavior of the hexagonal free form shell supported on six vertices subjected to wind loads. The analysis of structures of exceptional geometry subjected to wind loads is not widespread and it becomes necessary to determine the pressure distribution through the combined analysis of wind tunnel test and computer simulation results. Firstly, the computer program developed by Vizotto (2010) was used in order to create optimized shell geometries using a process that combines finite element methods and programming techniques. The generated shapes was used to build scale models. Internal and external pressure coefficients were obtained in a wind tunnel using the shell physical models subjected to laminar and turbulent flow regime. The analysis considers the most important wind load combinations with wind direction variations on open and closed sides. Finally, by means of computational fluid dynamics using the ANSYS computer simulation software package with the SST turbulence model, computational analysis was performed simulating wind flow conditions and the effect on the structure, ultimately comparing the results with those obtained experimentally.*



***Keywords:*** *Free form shells, Wind tunnel, Pressure coefficients, Computational fluid dynamics*

# 2 INTRODUCTION

Mother Nature has created multiple examples of shell type structures, e.g. sea shells, egg shells or the human skull among many others. All of them share the main property of having a very thin wall with respect to all other physical dimensions as well as presenting heavy resistance to compression (Roth, 2007). Therefore, the main objective of the research in the area of shell type geometries is to generate sustainable civil designs in the fields of design, materials and building methodologies that will guarantee a balance between the requirements for which they were conceived, people's comfort, environmental impact and the harmony with the space where they are located (Addis, 2001).

According to Pfluger (1965), shell type structures are defined as support structures, continuous, static and three dimensional with a curved variable surface. This solid structure is delimited by two surfaces and is especially characterized by having a considerably thin wall in relation to the other two dimensions of the surface, for which they could be considered as two dimensional elements (Khalil, 1976). Structurally, the shells support loads through membrane action, which depends on the geometry and the support conditions, mostly concentrating structural strains on the plane (Brandão, 2005).

As a result, free form shells are structures that resist loads due to their shape (Ramm and Mehlhorn, 1991), becoming very functional buildings capable of reaching big dimensions without the need for vertical elements in their interior, which makes them the ideal solution for amphitheater, sport or industrial venue designs (Isler, 1995). In addition to their architectural value, as they allow designers and engineers to experiment with diverse shapes with big visual impact due to their lightness compared with their dimensions, they also provide the added values of economy in the use of construction materials, luminosity and excellent acoustic and thermal behavior (Sena, 2008).

However, it is necessary to study thoroughly the behavior of these structures under wind loads (Taylor, 1991). As opposed to the case of heavy and robust constructions, wind loads can be a very important factor in the case of free form shell constructions because the presence of structural deficiencies due to high wind suction or pressure could be life threatening to the users (Block and Ochsendorf, 2007).

The objective of this paper is to make information and data available that could contribute to the analysis of the effect of wind loads in free form shell structures, both with experimental data on pressure coefficients obtained from atmospheric boundary layer wind tunnel tests using physical scale models (Laboratory of Environmental Comfort and Applied Physics – LaCAF at FEC-UNICAMP) as well as data obtained from ANSYS 14 fluid dynamics computer simulations recreating realistic conditions of the shell. These are tools that help increase the reliability of the structural engineer when considering wind loads because the insufficient availability of free form shell could lead the engineer to use rough or estimated data (Bletzinger et al., 2005), which could in turn generate incorrect pressure coefficients and ultimately lead to problems ranging from discomfort problems to structural damage (Patel, 1997).

# 3 SCALE MODELS AND WIND TUNNEL TESTS

## 3.1 Wind tunnel

The tests performed during this research were run in the atmospheric boundary layer wind tunnel at the Laboratory of Environmental Comfort and Applied Physics (LaCAF) at the School of Civil Engineering, Architecture and Urbanism of the University of Campinas, SP, Brazil.

The wind tunnel reaches a maximum speed of 20 m/s with a test section of 4.8 m x 0.9 m x 0.8 m (l x w x h) resulting in a 0.72 $m^2$ cross-section. It also has a 0.6 m diameter rotating disc for the containment of the model. Air gets into the tunnel through a 2.2 m x 1.95 m (w x h) aperture with two 1.5 mm square nylon mesh layers that reduce the big vortex providing a subsequent contraction that guarantees that the flow is laminar. The air then enters the test section and finally a fan sucks the air out of the tunnel (Matsumoto, 2008).

In order to simulate the turbulence conditions inside the tunnel, it is necessary to generate the profile of speeds of the atmospheric boundary layer. This is achieved with the construction of a panel made of PVC tubes and joints that send the wind in multiple directions. This panel is installed at the entry of the test section in order to create that required turbulence profile for the desired roughness.

**Figure 1. Wind tunnel and turbulence generating panel at LaCAF-FEC-UNICAMP**

The speed profile of the atmospheric boundary layer used by the LaCAF for different levels of roughness is given by the Eq. (1):

$$\frac{U_Z}{U_{ref}} = \left[\frac{z}{U_{ref}}\right]^{\alpha} \tag{1}$$

Where:

- U: average speed at height z;
- Uref: average speed at the reference height;
- α: exponent that varies according with the roughness under simulation, e.g. low roughness (α=0.1), mid (α=0.25) and high (α=0.4).

## 3.2 Modelling and instrumentation of scale models

The advantage of using scale models for the tests analysis is the fast acquisition of results for the study of structural behavior, viability of construction, effects and variations of the outer shapes (Maurin and Motro, 2004). It is imperative, however, to establish the conditions that must be met for the fluids around the scale object to be similar to those around the real object. In order to achieve this, the following must be taken into account; the geometric similarities of the objects, the kinematic similarities with respect to the same wind “structure” and the dynamic similarities that define the ratio of inertial forces to viscous forces (Blessmann, 1995).

The ratio of inertial to viscous forces is defined by Reynolds number, which only allows the comparison of fluids around geometrically similar and equally oriented objects (Smith and Wilson, 1971). Once these conditions are met, the ratio between pressures on similar points of the model and the real construction can be determined via the pressure coefficients, which are the same for the model and the real structure (Blessmann, 1995).

The free form shell was shaped by Ferreira (2013) with the same techniques developed by Vizotto (2010) using the ANSYS software package at the IT laboratory of the FEC-UNICAMP, where a thin membrane subject to its self-weight is simulated, restricting the displacements at the support points.

The dimensions used in the construction of the models must follow the geometric specifications of the test section inside the wind tunnel, where the object could obstruct up to a 7% of the total cross-section area in order to prevent rollover effect interference in the tests. Therefore, the models have an effective cross-section of 0.05 $m^2$ with a minimum distance of 20 cm between each side and the walls of the tunnel.

The models were constructed in the Automation and Prototype Laboratory for Architecture and Construction (LAPAC) at the School of Civil Engineering, Architecture and Urbanism (FEC) of the University of Campinas (UNICAMP). The milling machine CNC MTC Robotic (Taz), with a cutting section of 1500 mm x 2300 mm, was used together with the numerically generated models to sculpt the high density polystyrene pieces that were used as molding tools to build the fiberglass scale models with the dimensions presented in Figure 2, with obstruction area of 478.45 $cm^2$ (6.64 %).

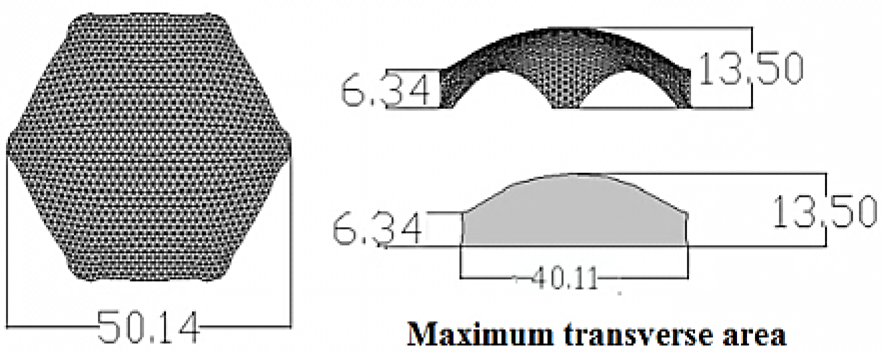


**Figure 2. Dimensions of the scale model of hexagonal free form shell (cm)**

Two identical scale models were built for the measurement of the external and internal pressure coefficients respectively, with each model being divided into 61 areas where pressure measurements were performed. Properly numbered holes were made in each of these areas in order to install hoses with 1mm internal and 1.6 mm external diameters, which were then connected to the pressure scanner of the wind tunnel for data readings and collection (Ferreira, 2013).

Once the hoses were installed, the models were placed on a wooden circular base of 16 mm thickness with the same diameter of the fixing base of the wind tunnel. In order to measure the external pressure coefficient, the hoses go underneath the base at the lower outer part of the tunnel so they do not interfere with the outer surface of the structure. In order to measure the internal pressure coefficient, the hoses go over the outer top side of the structure to prevent them from being fixed to the higher side of the tunnel and obstructing the data readings for the inner surface of the shell, according to Figure 3.

**Figure 3. Plastic hoses connected to the scanner for external and internal pressure measurement**

In order to perform the analysis of the internal pressure coefficients, the recommendations and concepts of the Brazilian Standard NBR-6123 were used as reference – wind loads on buildings type item 6.2.5, alluding to the internal pressure coefficients from wind load effects, which illustrates the variations of the predominant aperture and its position with respect to windward blowing winds. The apertures of the scale model were closed with rigid blue polyethylene sheets of 3 mm thickness attached to the structure with silicon that guarantee impermeability and facilitate the removal of the sheet for the various combinations of tests.

## 3.3 Wind tunnel tests

The positions of the scale model in the tunnel were chosen in accordance with the recommendations and concepts of the NBR-6123 that refer to the most critical combinations of predominant aperture with respect to the direction of the wind against the structure. The number of tests and the combinations of aperture and wind direction against the structures were defined considering the symmetry axes of the hexagonal shell.

The tests performed for the measurement of pressures outside and inside of the structure were divided into three critical cases of predominant aperture and each test was evaluated for laminar and turbulent flow regimes:

1. Totally closed structure subject to wind loads at 0º and 90º;
2. Structure with predominant aperture subject to windward (0º) and leeward (180º) wind loads;

3. Structure with two predominant apertures, subject to windward wind load (0º) and loads parallel to the aperture (90º).

The measurement of the pressure on each of the 61 reading points of the models was made using a 64 channel pressure scanner and the obtained data was stored in a text file. Each test produced 100 data samples per second during two minute periods for each one of the following engine frequencies defining the speed of the wind (130, 230, 330, 430, 530, 630, 730 and 830 rpm) with a maximum speed of 20 m/s. The information is compiled in a .txt file formed of 62 columns, 61 of which represent the data for each point with the last one representing the Pitot tube. The function of the Pitot tube is to measure the reference static pressure inside the tunnel and is positioned opposite to the model, bent and aligned with the flow at a height of 53 cm.

In order to generate turbulence inside of the tunnel and generate a wind speed profile equivalent to a low roughness area with α=0.2, a panel with white 50 mm PVC joints was used as shown in Fig. 1.

The calculation of the dimensionless value of the pressure coefficient was made considering the dynamic relationship between the wind and the pressure applied on the sides of the structure (Melbourne, 1993). Using the data stored in the file generated by the scanner, the coefficients for each test were calculated as the division of the average value of the pressure for each point by the value of the reference pressure of the Pitot tube as shown by the Eq. (2) and Eq. (3) (Faghih and Bahadori, 2009).

$$cp = \frac{p - pref}{pdinamica} \tag{2}$$

$$cp = \frac{p - p_0}{\frac{1}{2}\,\rho\, v_0^2} \tag{3}$$

Where:

- Cp: pressure coefficient (dimensionless);
- p: pressure read at each point (Pa);
- pref = po: static pressure at a flow point un-perturbed by the scale model;
- ρ: air density inside of the wind tunnel (kg/m$^3$);
- Vo: wind speed before hitting the scale model (m/s);
- Pdinamica $= \frac{1}{2}\,\rho\, v_0^2$ : dynamic reference pressure of the Pitot tube.

With the calculation of the pressure coefficients for each engine rotation speed, it can be observed that the coefficient value stabilizes as the speed increases producing the average value that is used in the analysis.

Finally, the pressure coefficients for each point are obtained, which are used to generate the graphs of isobaric pressure lines on the surface of the structure for which the freeware software package TopoCal 2005 was used (http://www.topocal.com).

# 4 COMPUTATIONAL FLUID DYNAMICS

The availability of high speed and high storage computers in the 20th and 21st centuries has enabled researchers and engineers to solve complex problems using numeric and algorithmic analysis techniques. One such tool is the Computational Fluid Dynamics (CFD), which provides a numerical solution to the Navier-Stokes differential equations that define the transport of mass, momentum and energy in the motion of fluids in a specific domain, space and time (Melarano, 1982).

Notwithstanding this, the empiric information of the tests run in different areas that has been gathered in manuals and tables throughout the years, has helped researchers to validate the numeric models with real data. Given that the new simulations that attempt to illustrate a particular phenomenon need to relate to and be validated with experimental data, it must be remembered that numeric models always present approximate data with differences with respect to real results, errors that must be within acceptable margins in order for the model to be used in the design (Maliska, 1995).

## 4.1 Turbulence model

Turbulence is defined as the wind oscillation around a measure and is a property of the flow and not the fluid, where fast pressure and speed changes are present in the space and time domains. Turbulence can also be understood as the group of whirlwinds of different sizes hat form the flow (Cheung and Melbourne, 1983).

There are various turbulence models available like the LES (Lage Eddy Simulation), but their academic use is still not feasible because they need large computational processing power. Models obtained from the use of the Reynolds number and the Navier-Stokes equations, called Reynolds Averages Navier-Stokes equations (RANS), which have different levels of sophistication, or the Reynolds Stress equation (RMS), which treats turbulence in each direction separately, arose afterwards. There are also turbulence models called of first order that simplify the problem using two equations to discover the phenomenon, which makes up for faster simulations (Maliska, 1995).

This research uses the SST model, which is a RANS type model that uses the equations of the k-ε and k-ω models. In the outer area of the flow, it uses the equations of the k-ε model and in the area next to the wall (Savory and Toy, 1986), where this model is deficient; it uses the transport equations of the k-ω model. The SST model uses two transport equations, one of which is the turbulent kinetic energy (Eq. 4) and the other is the specific dissipation rate of turbulent kinetic energy (Eq. 8) (Martins, 2012).

$$\frac{\partial k}{\partial t}+\frac{\partial v_i k}{\partial x_i}=\frac{\tilde{P}_k}{\rho}-\beta^{*}\omega k+\frac{1}{\rho}\frac{\partial}{\partial x_i}\left[\,(\mu+\sigma_k\,\mu_t)\;\frac{\partial k}{\partial x_i}\,\right] \tag{4}$$

Where:

- $v_i$ : velocity components;
- ρ : specific mass;
- μ : molecular viscosity;

- $\mu_t$ : turbulent viscosity;
- $\tilde{P}_k$: production limiter used in in the stainless action model to prevent turbulence accumulation in the blockage area.

$$\tilde{P}_k = min(P_k 10\varepsilon) \tag{5}$$

$$\varepsilon = \beta^* \omega k \tag{6}$$

$$P_k = \mu_t \frac{\partial v_i}{\partial x_j}\left[\frac{\partial v_i}{\partial x_j} + \frac{\partial v_j}{\partial x_i}\right] \tag{7}$$

The turbulent kinetic energy dissipation rate equation (ω), in accordance with the SST model is given by the following expression (Menter et al., 2003):

$$\frac{\partial \omega}{\partial t} + \frac{\partial v_i \omega}{\partial x_i} = \alpha S^2 - \beta^* \omega^2 + \frac{1}{\rho}\frac{\partial}{\partial x_i}\left[(\mu + \sigma_\omega \mu_t)\frac{\partial \omega}{\partial x_i}\right] + 2(1 - F_1)\,\sigma_{\omega^2}\frac{1}{\omega}\frac{\partial k}{\partial x_i}\frac{\partial \omega}{\partial x_i} \tag{8}$$

Where function $F_1$ equals to 1 in the region close to the wall (activating the original k-ω model) and is null far away from the wall (k-ε model). The combination with the k-ω model is made in the region of the boundary layer (Cebeci, 2004). The functions $F_1$ and $CD_{kw}$ are defined in the Eq. (9) and Eq. (10).

$$F_1 = \tanh\left[\left[min\left[max\left[\frac{\sqrt{k}}{\beta^* \omega y}; \frac{500v}{y^2\omega}\right]; \frac{4\rho\sigma_{\omega^2} k}{CD_{k\omega} y^2}\right]\right]^4\right] \tag{9}$$

$$CD_{k\omega} = max\left[2\rho\sigma_{\omega^2}\frac{1}{\omega}\frac{\partial k}{\partial x_i}\frac{\partial \omega}{\partial x_i}, 10^{-20}\right] \tag{10}$$

Where:

- y : distance between the surface and the wall;
- and the other constants are those of the k-ε and k-ω models, i.e.

$$\beta = 0.009;\ \alpha_1 = 5/9;\ \beta_1 = 3/40;\ \sigma_\omega = 0.5;\ \sigma_{\omega^2} = 0.856;\ \beta_2 = 0.0828;\ \alpha_2 = 0.44$$

The turbulent viscosity is calculated using this model as Eq. (11):

$$\mu_t = \rho \frac{\alpha_1 k}{max\left[\alpha_1 \omega \left(S_{ij} S_{ij}\right)^{1/2} F_2\right]} \tag{11}$$

Where:

- $\left(S_{ij} S_{ij}\right)^{1/2}$ : is a measure of the strain rate tensor;
- $F_2$: is a combination of functions in the boundary layer determined by Eq. (12):

$$F_1 = \left[\tanh\left[max\left[\frac{2\sqrt{k}}{\beta^* \omega y}; \frac{500v}{y^2 \omega}\right]\right]^2\right] \tag{12}$$

## 4.2 Numerical method

The evaluation of the problem comes as the simultaneous resolution of the equations presented above through numerical analysis techniques. Simulations were made through CFD analysis, using the ANSYS CFX 14 software package, which uses finite volume approach (FVA) to resolve the transport differential equations. The basic hypotheses adopted by the model are:

- There is only one phase;
- Laminar or turbulent flow;
- Incompressible flow;
- Isothermal system.

Boundary conditions are fundamental in the resolution of the Navier-Stokes non-linear partial differential equations, given that they restrict each of the boundaries of the simulated domain. The limits of the domain can be configured as walls and apertures. Walls are the borders that prevent the entry and exit of fluid in and out of the domain. Walls can be classified into two groups, depending of the acting loads; namely “no slip” and “free slip”. This classification allows the differentiation between the real walls of the object and the domain floor, which receive zero velocity, and the domain walls and ceiling, which are under load (Pasqual, 2011).

Real walls are used to generate the mesh used for the simulation of the boundary layer, which establishes that the flow adhere to the solid boundary producing a null velocity in these regions. On those walls considered without loads there is no boundary layer because the fluid does not adhere to the solid and the boundary effects diminish in the simulation (Munson et al., 2012). Moreover, it is necessary to define the boundaries through which the fluid will enter and leave the domain, which are configured as “inlet” and “outlet” respectively.

For the laminar flow simulations, the entry walls of the domain were configured as “inlet”, with an initial wind speed (U) of 20 m/s. The back side of the parallelepiped is called “outlet” on which a static pressure of 1 atmosphere is defined. The side walls of the domain, and the structure floor and walls are configured as zero-velocity walls, for which the mesh of the boundary layer was made. The domain created for the laminar flow regime has the same dimensions as the LaCAF wind tunnel, because it is necessary that the wind develops the same velocity profiles and reaches the structure in the same experimental conditions.

On the other hand, for the turbulent flow regime simulations, the entry wall of the domain, “inlet” is configured according to the velocity profile equation defined by Matsumoto (2008). The back side of the domain is also called “outlet” as in the case of the laminar flow regime. The side walls of the domain are configured as walls under load given that the velocity profile is known which makes it unnecessary to generate a domain with the same dimensions as the wind tunnel. Finally, the structure floor and walls are configured as zero-speed walls. Figure 4 show the domain conditions in the laminar and turbulent flow regimes respectively.

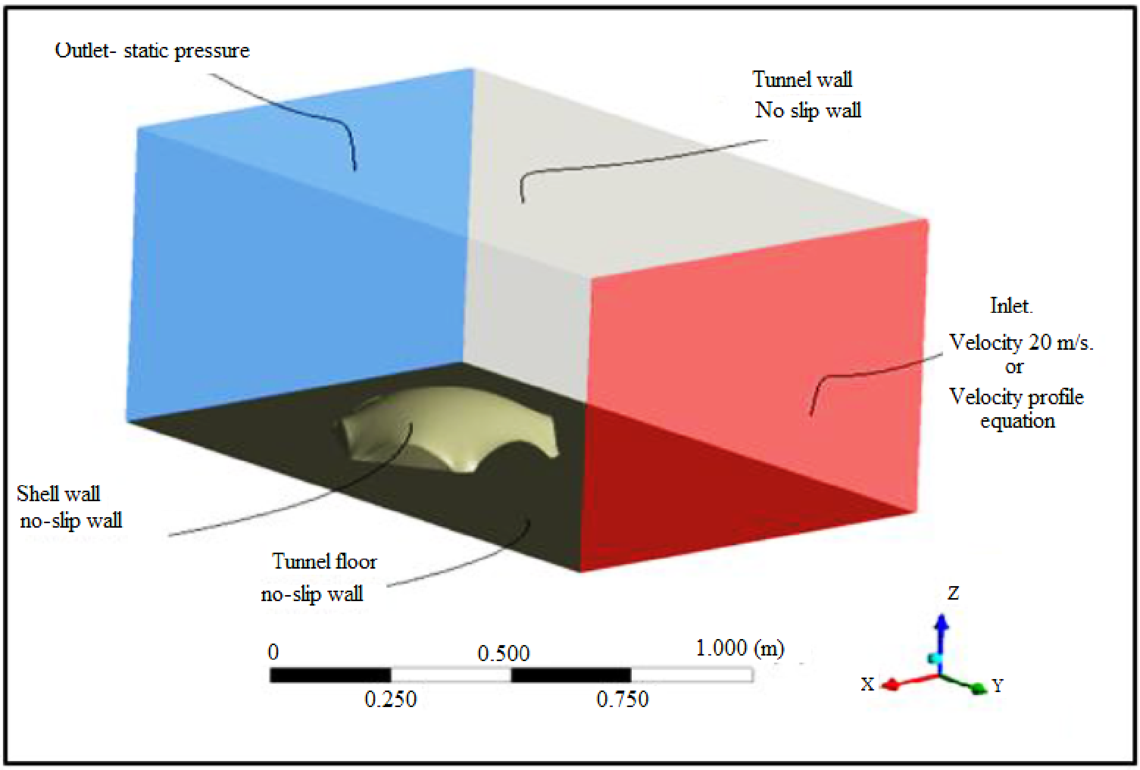


**Figure 4. Domain and boundary conditions of the shells in the wind tunnel (laminar and turbulent flow)**

Tables 1 and 2 describe the boundary conditions for laminar and turbulent flow regimes respectively, while Table 3 presents the air physical properties and characteristics.

**Table 1. Boundary Conditions – Laminar Flow Regime**

| Region | Boundary Condition Laminar Flow Regime | | CFX condition |
|---|---|---|---|
| Entry | Prescribed Velocity | 20 m/s | Velocity |
| Exit | Prescribed Pressure | 1 atm | outlet-static pressure |
| Tunnel Walls | Velocity | 0 m/s | no-slip wall |
| Tunnel Floor | Velocity | 0 m/s | no-slip wall |
| Shell Walls | Velocity | 0 m/s | no-slip wall |

**Table 2. Boundary Conditions – Turbulent Flow Regime**

| Region | Boundary Condition Turbulent Flow Regime | | CFX condition |
|---|---|---|---|
| Entry | Velocity Profile | - | (Matsumoto, 2008) |
| Exit | Prescribed Pressure | 1 atm | outlet-static pressure |
| Tunnel Walls | Free Wall | 0 m/s | free-slip wall |
| Tunnel Floor | Velocity | 0 m/s | no-slip wall |
| Shell Walls | Velocity | 0 m/s | no-slip wall |

**Table 3. Physical Properties of Air**

| | | | |
|---|---|---|---|
| Temperature | T | 25 | °C |
| Specific Mass | P | 1.184 | kg/m$^3$ |
| Dynamic Viscosity | M | 1.85 | (N·s/m$^2$) 10$^{-5}$ |
| Kinematic Viscosity | N | 1,.6 | (m$^2$/s) 10$^{-5}$ |
| Thermal Conductivity | Λ | 0.024 | W/(m·K) |
| Specific Heat | C | 1012 | J/(kg·K) |

## 4.3 Mesh generation

In order to generate the mesh of the boundary layer, the near region to the walls is considered, where big pressure gradients exist at the same time that the viscous effects in this zone are also considerable (Varma and Kanann, 2005).

In order to guarantee a solution to the boundary layer it is crucial to define criteria like the minimum width between nodes of the boundary layer as wells as the number of nodes (Costola, 2006). This research is based on the generation of a tetrahedral mesh with the parameters presented in Table 4.

**Table 4. Mesh Parameters**

| | | |
|---|---|---|
| Mesh Method | Tetrahedral | |
| Boundary Layer Thickness | 0.004 | [m] |
| First Layer Height | 0.000018 | [m] |
| Number of Layers | 15 | |
| Maximum Element Size | 0.001 | [m] |
| Mesh Elements | 7,000,000 | |

In the simulation, calculations were made iteratively in a transient state. During the calculation process the program allows the verification of the solution by monitoring the variables, in this case the pressure coefficient. It was programmed in such a way that the simulation was concluded when this particular variable reached a stable average value, (Moreno, 2012).

Simulations were made using a 12 2.4 GHz Intel Xeon processor CPU with 12 GB RAM memory. A 5 second time step and an Error Root Mean Square (RMS) minimization were used as convergence criterion (maximum value $10^{-4}$). Figure 5 show the generated mesh and the detail of the boundary layer.

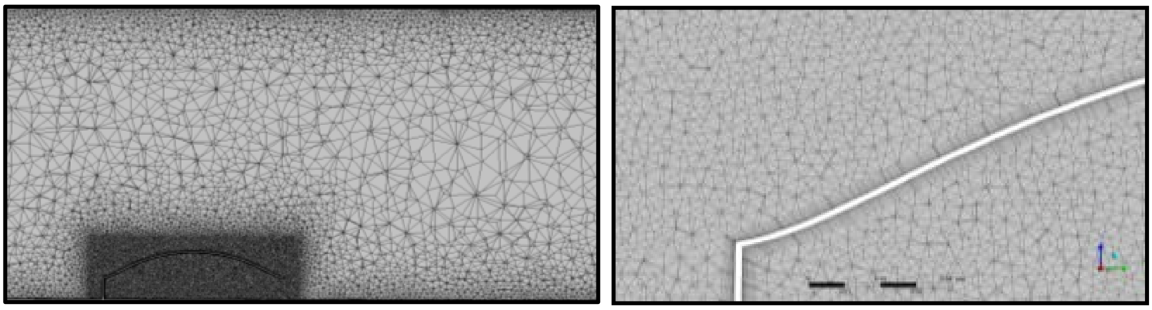

**Figure 5. Transversal section and detail of the mesh in the region of the boundary layer**

Finally the computer model of the fluid was obtained, where the current lines and vertices can be observed through the shell as showed in Figure 6. The variables of the study are also calculated in order for them to be observed together with the experimental data.

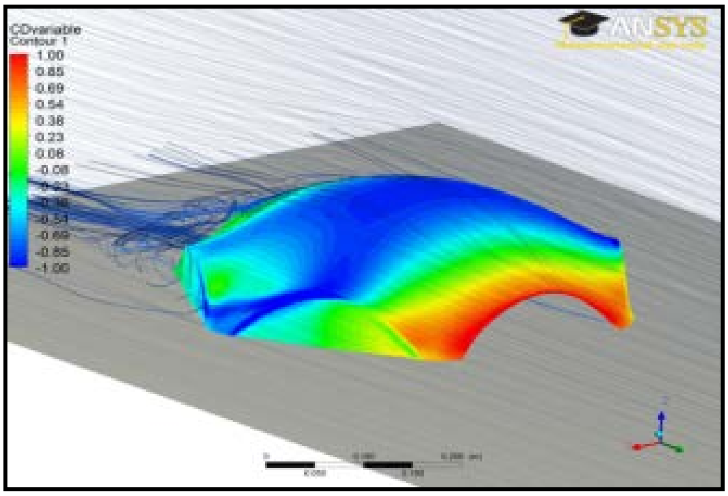

**Figure 6. Airflow on the structure with one aperture at windward in laminar regime**

# 5 RESULTS

The results were obtained for the both ANSYS computer model and experimental wind tunnel tests for the most critical cases of over-pressure and suction.

The total coefficients were obtained from the difference between the internal and external pressure coefficients for each point of the structure:

- Hexagonal shell with aperture and wind load in the windward direction at 0° in turbulent flow regime. Maximum suction with Cp value of (-1.7);
- Hexagonal shell with two parallel apertures and wind loads in the windward direction at 0° and turbulent flow regime. Maximum over-pressure with Cp value of (+1.2).

Numerical models were processed separately for the calculation of the external and internal pressure coefficients in the laminar and turbulent flow regimes for the presented cases, as showed in Fig. 7 to 14.

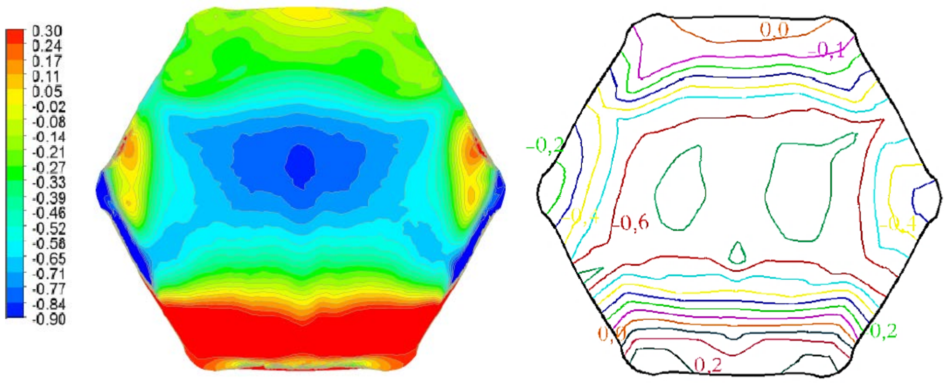


**Figure 7. External pressure coefficients on the shell with one aperture (ANSYS & Wind Tunnel) Wind load at windward direction at 0° in laminar flow**

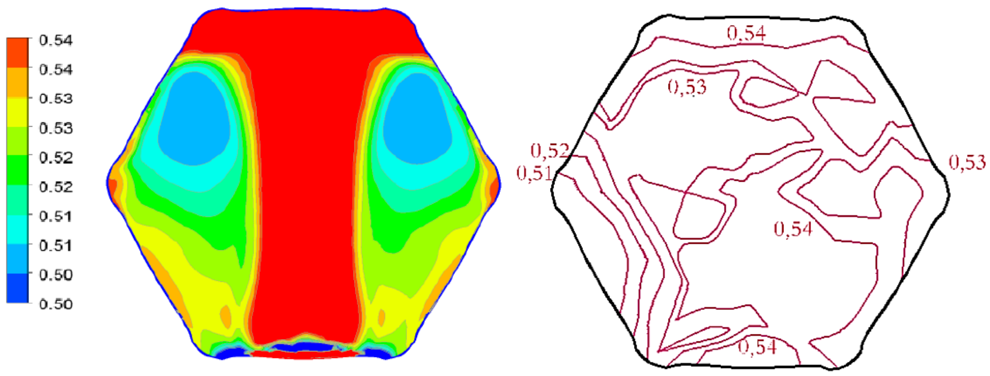

**Figure 8. Internal pressure coefficients on the shell with one aperture (ANSYS & Wind Tunnel) Wind load at windward direction at 0° in laminar flow**

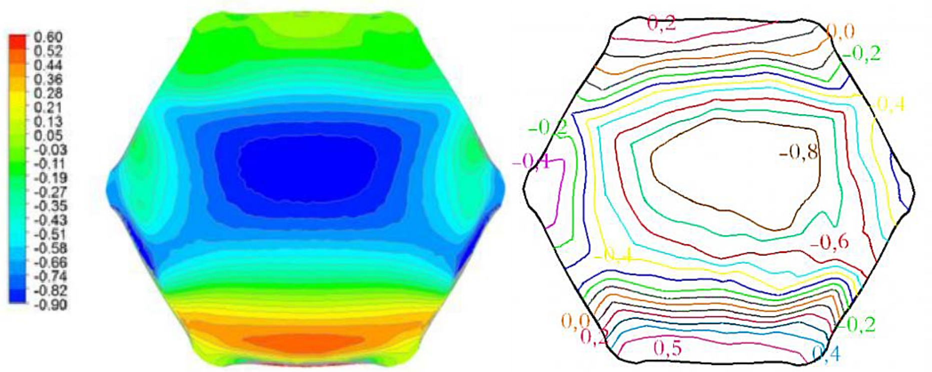

**Figure 9. External pressure coefficients on the shell with one aperture (ANSYS & Wind Tunnel) Wind load at windward direction at 0° in turbulent flow**

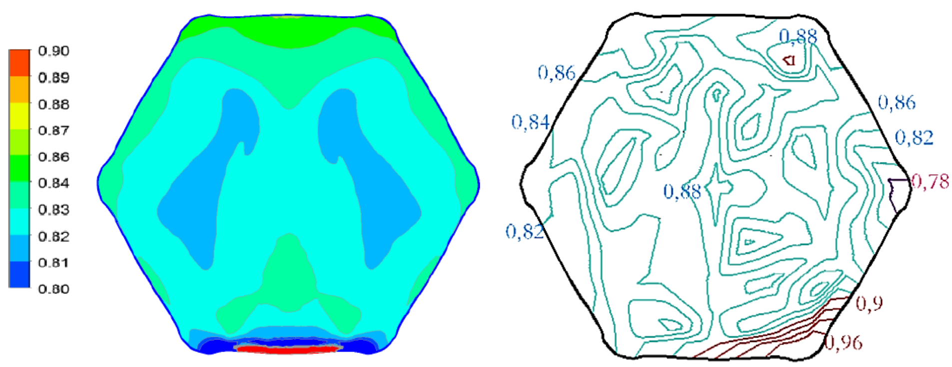

**Figure 10. Internal pressure coefficients on the shell with one aperture (ANSYS & Wind Tunnel) Wind load at windward direction at 0° in turbulent flow**

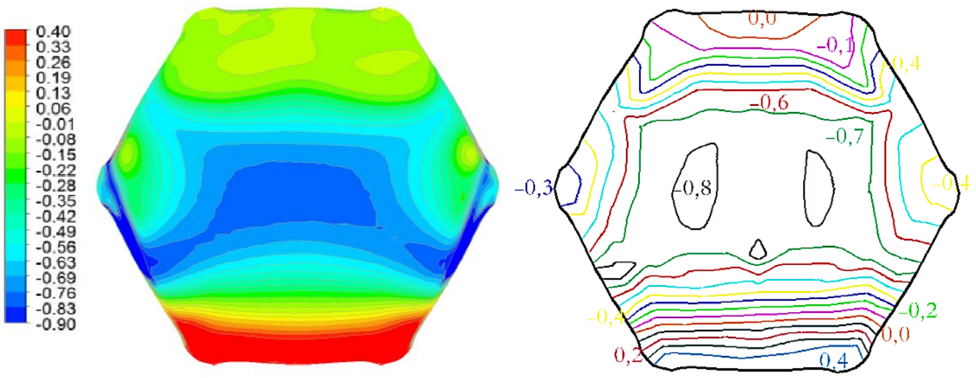


**Figure 11. External pressure coefficients on the shell with two apertures (ANSYS & Wind Tunnel) Wind load at windward direction at 0° in laminar flow**

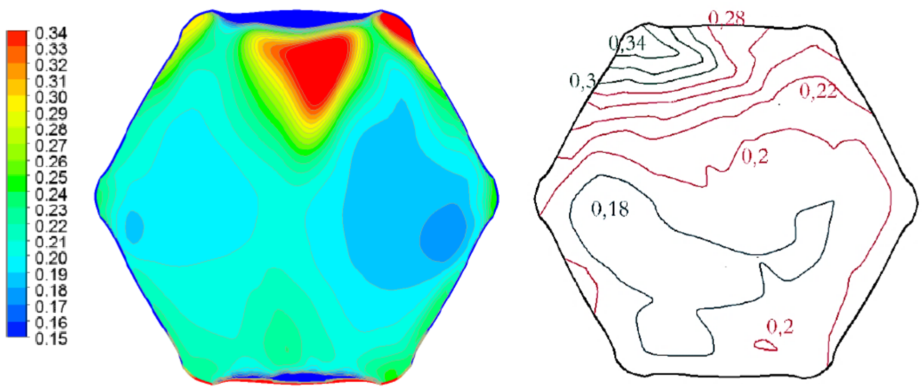


**Figure 12. Internal pressure coefficients on the shell with two apertures (ANSYS & Wind Tunnel) Wind load at windward direction at 0° in laminar flow**

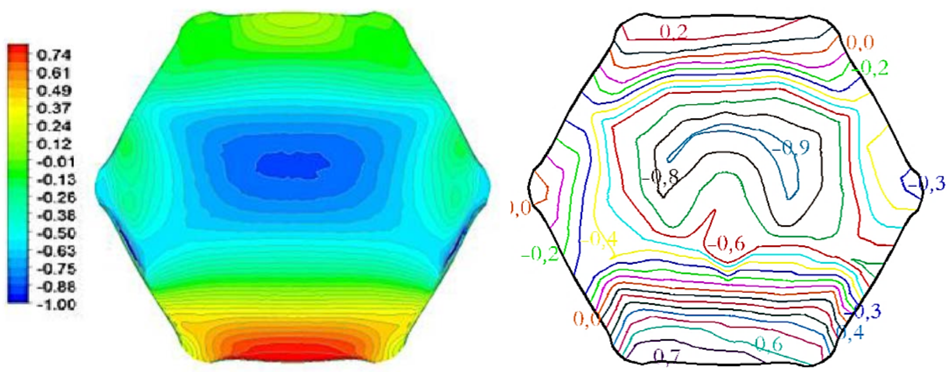


**Figure 13. External pressure coefficients on the shell with two apertures (ANSYS & Wind Tunnel) Wind load at windward direction at 0° in turbulent flow**

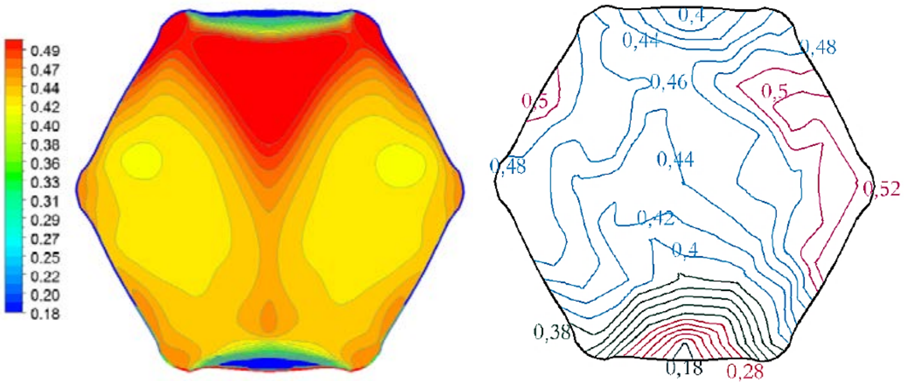


**Figure 14. Internal pressure coefficients on the shell with two apertures (ANSYS & Wind Tunnel) Wind load at windward direction at 0° in turbulent flow**

# 6 CONCLUSIONS

The comparison of the both numerical and experimental data certifies that there are a lot of similarities with small margins of error, in the order of 3% to 10%, whereas bigger errors are encountered in regions where there is a separation in the boundary layer delimiting the pressure and suction zones.

Therefore, computer models can be used in order to design free form shell structures and evaluate their behaviour under wind loads, with the advantage that any shape/form can be generated without the limitation of having to build complex physical scale models. Thus, it is possible to avoid the high costs of wind tunnel tests, enabling the analysis of a bigger number of wind directions, the evaluation of the environmental impact, the presence of neighboring buildings, etc.

# ACKNOWLEDGEMENTS

I would like to show my appreciation to the work team: Prof. Dr. Isaias Vizotto, my colleagues Eng. Sebastián Moreno and Dr. Antônio Mário Ferreira; Prof[a]. Dr.[a] Lucila Chebel Labaki, Dr. Edson Matsumoto and to CAPES Foundation, Ministry of Education of Brazil, for having funded this research.

# REFERENCES

Addis, W., 2001. Creativity and innovation: the structural engineer's contribution to design. *Architectural Press*. Oxford.

Associação Brasileira de Normas Técnicas. NBR-6123, 1998. *Forças Devidas ao Vento em Edificações*. Rio de Janeiro.

Blessmann, J., 1995. Pressures on domes with several wind profiles. *Wind Effects on Buildings and Structures*, pp. 317–326.

Bletzinger, K. U., Wüchner, R., Daoud. F., & Camprubí, N., 2005. Computational Methods for Form Finding and Optimization of Shells and Membranes. *Computer Methods in Applied Mechanics and Engineering*, 194 (30–33), pp. 3438–3452.

Block, P. & Ochsendorf, J., 2007. Thrust Network Analysis: A New Methodology for Three-Dimensional Equilibrium. *Journal of the International Association for Shell and Spatial Structures*, 48 (3) pp. 167–173.

Brandão, J. H., 2005. *Análise experimental e numérica de cascas de concreto de ultra-alto desempenho reforçado com fibras*. PhD thesis, Universidade Federal do Rio de Janeiro/ Rio de Janeiro.

Cebeci, T., 2004. Turbulence Models and Their Application Efficient Numerical Methods with Computer Programs. Horizons Publishing Inc., Long Beach/California.

Cheung, J. C. K., & Melbourne, W. H., 1983. Turbulence effects on some aerodynamic effects of a circular cylinder at supercritical Reynolds numbers. *Journal of Wind Engineering and Industrial Aerodynamics*, 14 pp. 399–410.

Costola, D., 2006. V*entilação por ação do vento no edifício: procedimentos para quantificação*. MSc. Thesis. Escola de Arquitetura e Urbanismo da USP/São Paulo.

Faghih, A. K., & Bahadori, M. N., 2009. Experimental Investigation of Air Flow Over Domed Roofs. *Iranian Journal of Science & Technology, Transaction B, Engineering*. School of Mechanical Engineering, Sharif University of Technology, Vol. 33, No. B3, pp 207–216. Tehran, I. R./ Iran.

Ferreira, A. M., 2013. *Estruturas em Cascas de Formas Livres sob Ação do Vento*. PhD thesis, UNICAMP/Campinas.

Isler, H., 1995. 50 Years of Shells, In: Obrębski J.B. *International Conference on Lightweight Structures in Civil Engineering*, magat®, Magdalena Burska, Warsaw, pp. 31–42.

Khalil, M., 1976. *Contribuição ao cálculo das cascas de revolução mediante diferenças finitas*. MSc thesis. Universidade de São Carlos/São Paulo.

Maliska, C., 1995. *Transferência de calor e mecânica dos fluidos computacional: fundamentos e coordenadas generalizadas*, Livros Técnicos e Científicos/Rio de Janeiro.

Martins, R., 2012. *Biomimética no projeto de estruturas espaciais*. MSc thesis, Universidade Nova de Lisboa/ Portugal.

Matsumoto, E., 2008. *Calibração do túnel de vento de camada limite atmosférica e ensaios de aberturas em edificações utilizando modelos reduzidos*. UNICAMP/Campinas.

Maurin, B., & Motro, R., 2004. Concrete Shells Form-Finding with Surface Stress Density Method. *Journal of Structural Engineering*, 130 (6) pp. 961–968.

Melarano, M., 1982. *Wind in Architectual Desing*. Van Nostrand Reinhold Company/Nova York.

Melbourne, W. H., 1993. Turbulence and the leading edge phenomenon. *Journal of Wind Engineering and Industrial Aerodynamics*, Vol. 49, Issues 1–3, pp. 45–63.

Menter, F. R., Kuntz, M., & Langtry, R., 2003. *Ten Years of Industrial Experience with the SST Turbulence Model*. Software Development Department, Turbulence, Heat and Mass Transfer, ANSYS – CFX, 83714 Otterfing, Germany.

Munson, B. R., Young, D. F., & Okiishi, T. H., 2012, *Fundamentos da mecânica dos fluidos*. Blucher.

Moreno, S., 2012. *Avaliação fluidodinâmica do HDT em regime contracorrente com o uso da fluidodinâmica computacional – CFD.* MSc. Thesis. Faculdade de Engenharia Química da Unicamp/Campinas.

Pasqual, S., 2011. *Um estudo sobre a ação do vento nas estruturas de membrana*. MSc. Thesis. Escola Politécnica da USP/ São Paulo.

Patel, D. P., 1997. *An Experimental Analysis of Wind Stress in Shells*. Brigham Young University. 1969. Economics, pp. 345-354. Nanyang Technological University/Singapore.

Pfluger, A., 1965. *Estatica elemental de las cascaras*; trad. Renate Leisse de Mertig y Mario H. Buenos Aires.

Ramm, E., & Mehlhorn, G., 1991. *On Shape Finding Methods and Ultimate Load Analysis of Reinforced Concrete Shells, Engineering Structures* 13 (2), pp. 178–198.

Roth, L. M., 2007. *Understanding architecture: its elements, history, and meaning Boulder*, CO. Westview.

Savory, E. & Toy, N., 1986. Hemispheres and Hemisphere-cylinders in Turbulent Boundary Layers. *Journal of Wind Engineering and Industrial Aerodynamics*, 23, pp. 345–364.

Sena, C. F., 2008. Coberturas em betão armado e pré-esforçado solução estrutural tipo casca. MSc. thesis. Universidade Técnica de Lisboa/ Lisboa.

Smith, P. G., & Wilson, E. L., 1971. Automatic Design of Shell Structures. *ASCE Journal of Structural Division*, pp. 191–201.

Taylor, T.J., 1991. Wind pressures on a hemispherical dome. *Journal of Wind Engineering and Industrial Aerodynamics*, 40, pp. 199–213.

Varma, M. N., & Kanann, A., 2005. A. Enhanced food sterilization through inclination of the container walls and geometry modifications. *International Journal of Heat and Mass Transfer, Oxford*, v. 48, n. 18, pp. 3753–3762.

Vizotto, I., 2010. Computational Generation of Free-Form Shells in *Architectural Design and Civil Engineering, Automation in Construction*, Vol. 19, No. 8, pp. 1087–1105.